LETTERS

The purpose of this Letters section is to provide rapid dissemination of important new results in the fields regularly covered by Physics of Fluids. Results of extended research should not be presented as a series of letters in place of comprehensive articles. Letters cannot exceed four printed pages in length, including space allowed for title, figures, tables, references and an abstract limited to about 100 words. ***There is a three-month time limit, from date of receipt to acceptance, for processing Letter manuscripts. Authors must also submit a brief statement justifying rapid publication in the Letters section.***

Spectra of the very large anisotropic scales in turbulent channels

Juan C. del Álamo[a)] and Javier Jiménez[b)]
School of Aeronautics, Universidad Politécnica, 28040 Madrid, Spain

(Received 24 January 2003; accepted 7 March 2003; published 23 April 2003)

The spectra of numerically simulated channels at $\mathrm{Re}_\tau=180$ and $\mathrm{Re}_\tau=550$ in very large boxes are described and analyzed. They support a model in which the u-structures can be decomposed in two components. The first one is formed by structures of size $\lambda_x \gtrsim 5\,h$, $\lambda_z \approx 2\,h$, which span most of the channel height, and penetrate into the buffer layer. The second one has maximum intensity in the near-wall region, where it is highly anisotropic and scales in inner units. It widens, lengthens, and becomes more isotropic in the outer layer, where it scales with h. The cospectrum exhibits an analogous quasi-isotropic range, whose width grows linearly with wall distance. At the present Reynolds numbers, nothing can be said about a possible streamwise similarity, due to limited scale separation. An extensive set of statistics from the simulations is downloadable from ftp://torroja.dmt.upm.es/channels.
[DOI: 10.1063/1.1570830]

We discuss direct numerical simulations of the turbulent incompressible flow in plane channels at Reynolds numbers $\mathrm{Re}_\tau=180$ and $\mathrm{Re}_\tau=550$, based on the wall friction velocity, u_τ, and on the channel half-width h. Our emphasis will be on the comparison of the two numerical experiments. Following Kim *et al.*,[1] we integrate the Navier–Stokes equations in the form of evolution problems for the wall-normal vorticity ω_y and for the Laplacian of the wall-normal velocity $\phi=\nabla^2 v$. The spatial discretization is fully spectral, using dealiased Fourier expansions in the wall-parallel planes, and Chebychev polynomials in y. The temporal discretization is third-order semi-implicit Runge–Kutta, as in Moser *et al.*[2]

Table I summarizes the parameters of the present numerical experiments, together with those of previous comparable simulations.[2,3] Although those simulations had somewhat higher Reynolds numbers, we will show below that the present ones are the first in which the numerical box is large enough not to interfere with the largest structures in the outer flow. The streamwise periodicities of the boxes were chosen to be at least $L_x=8\pi\,h$ based on experimental evidence that these structures have lengths $5\,h$–$15\,h$.[4–6] Little information about their widths was available in the literature, and preliminary simulations in boxes of different sizes at $\mathrm{Re}_\tau=180$ and $\mathrm{Re}_\tau=550$ were used to adjust the spanwise periodicity to $L_z=4\pi\,h$.

The present results show that, in channels, the longest scales appear in the streamwise velocity u at $y=0.5h$, while the widest ones appear in the spanwise velocity w at the center of the channel. In order to quantify how much those scales are constrained by the size of the box, we calculated the fraction θ_x^u of the streamwise kinetic energy u'^2 contained in the very long wavelengths $\lambda_x=2\pi/k_x \geqslant L_x$ at $y=0.5h$, and the fraction θ_z^w of the spanwise kinetic energy w'^2 contained in the very wide wavelengths $\lambda_z=2\pi/k_z \geqslant L_z$ at the center of the channel. These are the scales which either do not fit in the box or do so only marginally. In the present $\mathrm{Re}_\tau=550$ simulation, $\theta_x^u \approx 0.2$ and $\theta_z^w \approx 0.1$, while in Moser *et al.*,[2] the size of whose box has been overlaid on the spectra in Figs. 1(c) and 1(d), $\theta_x^u \approx 0.5$ and $\theta_z^w \approx 0.4$. This suggests that the boxes of the previous simulations[2,3] were too small to represent the largest structures in the flow, and that even the present one is in some ways marginal, particularly in the streamwise direction.

Achieving stationary statistics in these very long boxes is fairly expensive, and our experience with test cases at $\mathrm{Re}_\tau=180$ indicates that at least 10 wash-out times are needed to have confidence in the statistics of the largest scales. The present statistics were collected for the times given in last column of Table I, after discarding initial transients.

Figure 1(a) displays linearly spaced isocontours of the premultiplied two-dimensional energy spectrum of the

TABLE I. Summary of cases. The resolution is measured in collocation points, and U_b is the bulk velocity.

	Re_τ	Δx^+	Δz^+	$\Delta y^+_{\max}$	L_x/h	L_z/h	tU_b/L_x
Moser *et al.* (Ref. 2)	590	7.2	3.6	7.2	2π	π	—
Abe *et al.* (Ref. 3)	640	8.0	5.0	8.2	6.4	2	—
Present	180	8.9	4.5	6.1	12π	4π	22
Present	550	8.9	4.5	6.7	8π	4π	10

[a)]Electronic mail: juanc@torroja.dmt.upm.es
[b)]Also at Center for Turbulence Research, Stanford University, CA 94305.

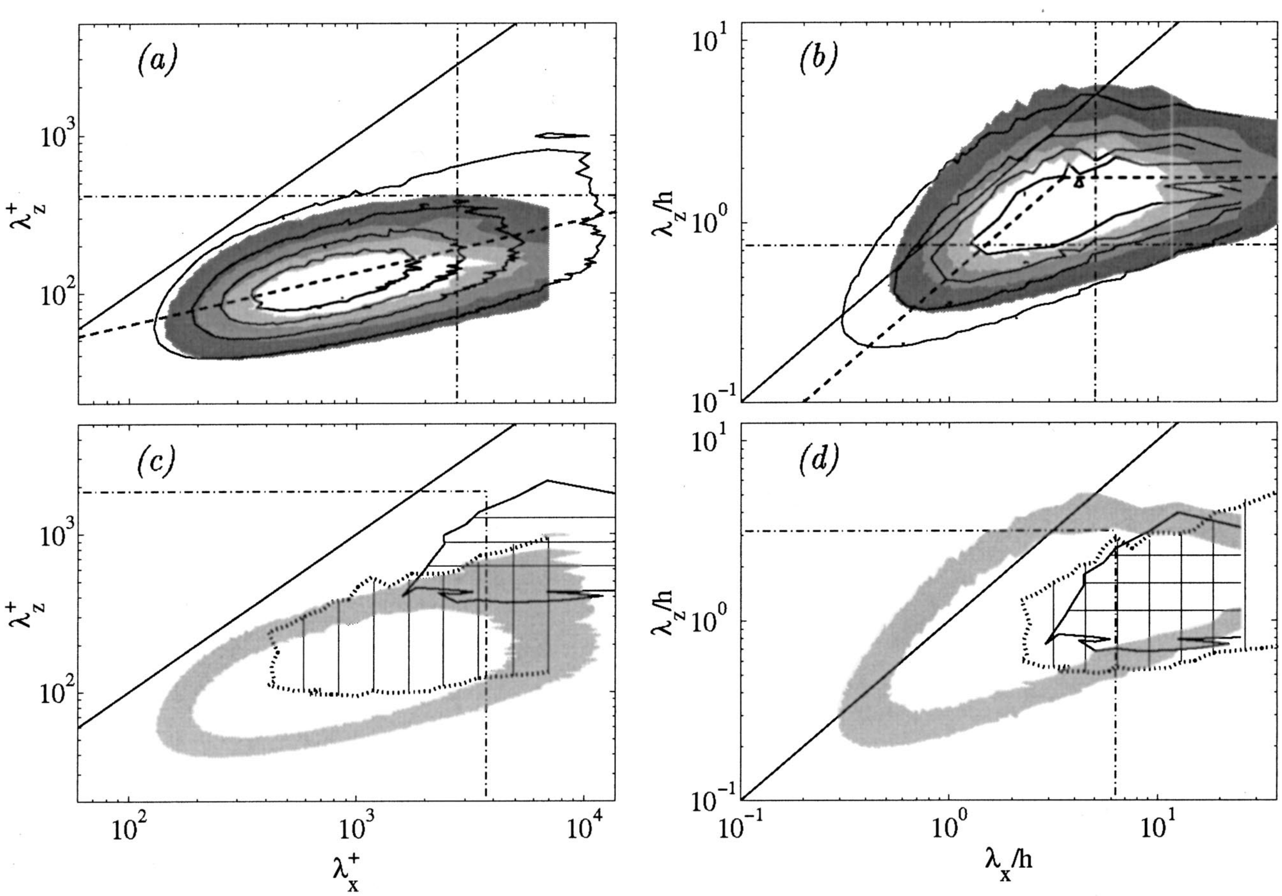

FIG. 1. (a), (b) Premultiplied two-dimensional spectra ϕ_{uu}/u_τ^2, as functions of λ_x and λ_z. Shaded contours, $Re_\tau=180$; line contours, $Re_\tau=550$. The contours are 0.2(0.2)0.8 times the common maximum value for both spectra at each wall-distance. The chain-dotted lines separate the bands of integration of the spectra in Fig. 2. The dashed straight lines in (a) have logarithmic slopes 1/3, while in (b) they represent $\lambda_x=2\lambda_z$ and $\lambda_z=1.75h$. (c), (d) The hatched patches are 15% contours of the two-dimensional spectral autocorrelation function ρ_{uu} between $y^+=15$, $y'/h=0.5$. Horizontal hatching, $Re_\tau=550$; vertical hatching, $Re_\tau=180$. The shaded areas lie between the two lowest contours of the $Re_\tau=550$ u-spectrum at the corresponding wall distances. The chain-dotted rectangles mark the size of the box in Moser *et al.* (Ref. 2). (a), (c) Inner units, $y^+=15$. (b), (d) Outer units, $y/h=0.5$. The solid straight lines are everywhere $\lambda_x=\lambda_z$.

streamwise velocity $\phi_{uu}=k_xk_z\langle\hat{u}(k_x,k_z,y)\hat{u}^*(k_x,k_z,y)\rangle$, where $\hat{u}$ is the Fourier coefficient of u, and k_x and k_z are the streamwise and spanwise wavenumbers. This spectral density measures the streamwise kinetic energy contained in a logarithmic wavelength interval centered at λ_x, λ_z. The line contours come from the simulation at $Re_\tau=550$, while the shaded ones are from the one at $Re_\tau=180$. The wall distance in the figure, $y^+=15$, is roughly the location of the near-wall peak of u'.

The u-spectrum in the near-wall region lies approximately along the power law $\lambda_x^+\sim(\lambda_z^+)^3$, implying that, while the structures of the streamwise velocity widen as they become longer, they also become more elongated, since they progressively separate from the spectral locus of two-dimensional isotropy $\lambda_x=\lambda_z$. This behavior is consistent with viscously-spreading similarity solutions of the linearized Squire's equation, under the assumption of a linear mean velocity profile and of a constant eddy viscosity in the near-wall region.[7]

There is still no general agreement about the scaling in the near-wall region. Contrary to the classical idea that inner scaling should work close enough to the wall, recent experimental evidence suggests that it does not,[4,8,9] and in particular that u'/u_τ increases with the Reynolds number throughout the wall layer at a fixed y^+. Some researchers[8,9] have argued that the Reynolds number dependence is due to the contribution of Townsend's[10] "inactive" motions. They note that this contribution scales in outer units, and are motivated by this observation to introduce a "mixed" scaling in which u'^2 is proportional to the product of the friction and outer velocities. Hites[4] presents a similar argument, but favors an interpretation in which the inner and outer contributions are scaled independently.

The present data agree with the latter idea. The only region of the two-dimensional u-spectra in Fig. 1(a) that does not collapse in wall units is their long-wavelength end. There is more kinetic energy there at $Re_\tau=180$ than at $Re_\tau=550$ for scales narrower than $\lambda_z^+\approx400$, while the opposite is true for wider scales. The reason for this incomplete scaling can be seen in Fig. 1(c), where the hatched patches represent the premultiplied two-dimensional autocorrelation function of the streamwise velocity

$$\rho_{uu}=|k_xk_z\langle\hat{u}(k_x,k_z,y)\hat{u}^*(k_x,k_z,y')\rangle|/[u'(y)u'(y')],\tag{1}$$

which can be understood as the spectral distribution of the

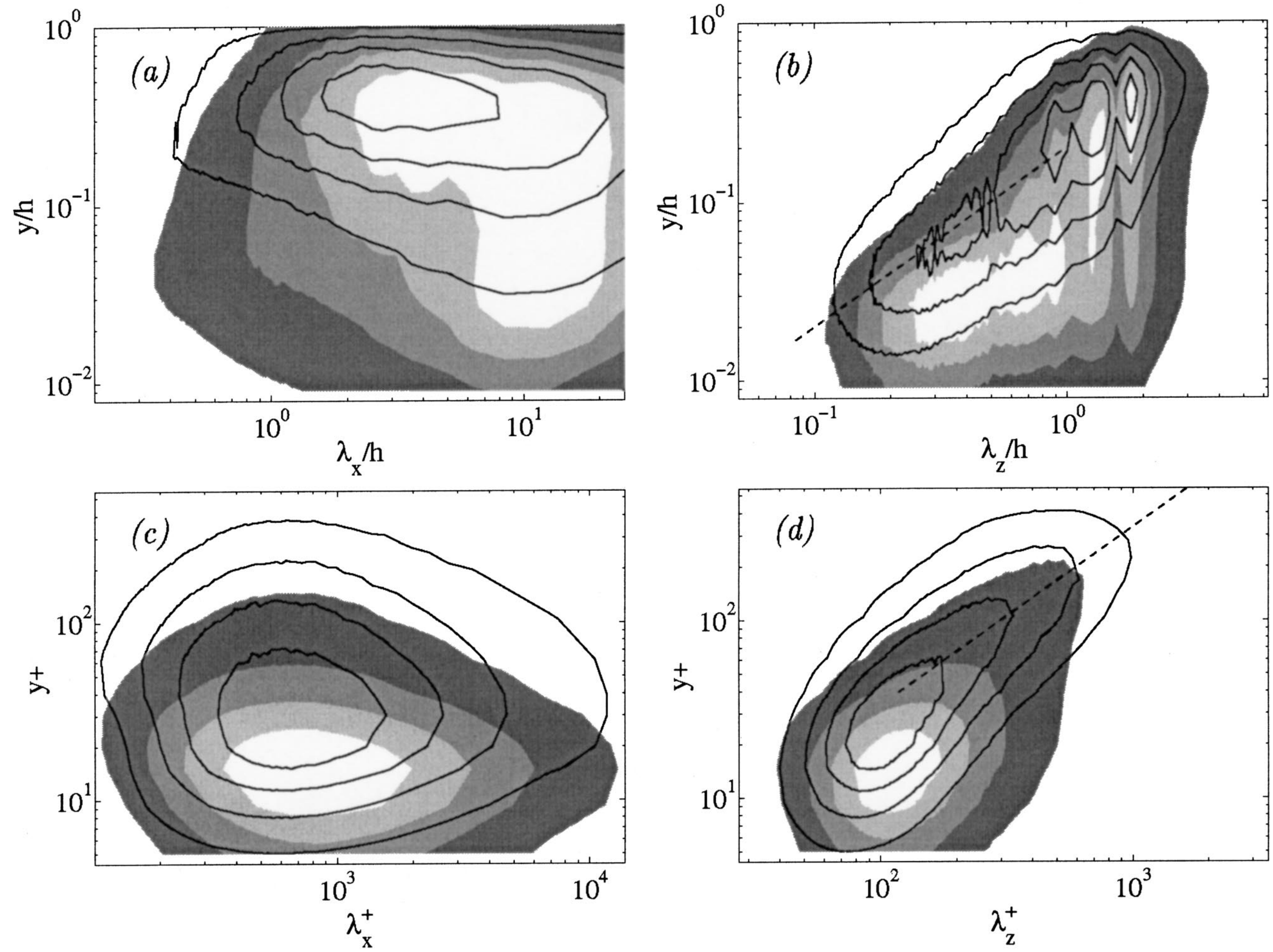

FIG. 2. Premultiplied one-dimensional spectra as functions of wavelength and wall distance, $Re_\tau=550$. Shaded contours, u-spectra; line contours, uv-cospectra. (a), (c) Streamwise spectra; (b), (d) spanwise spectra. The dashed straight lines have unit slope. (a), (b) Outer units; (c), (d) inner units. (a) Spanwise modes with $\lambda_z>0.75\,h$; (b) streamwise modes with $\lambda_x>5\,h$; (c) spanwise modes with $\lambda_z<0.75\,h$; (d) streamwise modes with $\lambda_x<5\,h$.

fraction of the streamwise kinetic energy that is correlated between y and y'. Note that the absolute value in the numerator of (1) defines the correlation function independently of the relative phases of the modes.

Figures 1(c) and 1(d) show the regions where the correlation ρ_{uu} between $y^+=15$ and $y'=0.5\,h$ is larger than 15% of its maximum. The shaded areas also included in those figures lie between the two lowest levels of the $Re_\tau=550$ u-spectrum, and have been added to allow comparisons of these plots with Figs. 1(a) and 1(b). For each of the two Reynolds numbers, the regions of high ρ_{uu} roughly coincide with the wavelengths in which there is an excess of streamwise kinetic energy in the near-wall region, suggesting that the latter is the result of the penetration into the buffer region of outer-layer structures. The integral of ρ_{uu} in wavenumber space is a measure of the fraction $C_u(y,y')$ of u'^2 which is correlated between the two heights. For the two wall-distances in Fig. 1, $C_u\approx0.15$, indicating that the penetration effect is strong. The fractions of the correlated energy for the other two velocity components are $C_v\approx0.01$ and $C_w\approx0.05$, in agreement with Townsend's[10] idea that the impermeability condition limits global contributions to the v-spectrum in the near-wall region, but not those to u and w.

The locations of the two hatched patches coincide when ρ_{uu} is represented in outer units [Fig. 1(d)], and they also coincide at both Reynolds numbers with the tails of ϕ_{uu} in the outer layer, which are located around $\lambda_x\gtrsim5\,h$, $\lambda_z\approx2\,h$. This suggests that the outer-layer u-structures can be decomposed into two types of modes. The first one would correspond to the hatched patches near the dashed horizontal line in Fig. 1(b). These modes are long anisotropic structures whose sizes scale with h, and which are very deep in the wall-normal direction. Long regions of uniform u' which extend from the near-wall region into the outer flow have been identified by Adrian *et al.*,[11] who argue that they may be the induced effect of coherent packets of hairpin vortices. The second class of modes forms a quasi-isotropic range which lies in Fig. 1(b) along the ridge $\lambda_x=2\,\lambda_z$. The location of the large-wavelength end of this ridge scales in outer units, while that of the short-wavelength end scales in inner units, so that the ridge becomes longer as the Reynolds number increases. Similar nearly-isotropic modes can be found along $\lambda_x=\lambda_z$ in the premultiplied spectra of v and w in the outer region (not shown). These quasi-isotropic modes of the three velocity components probably belong to the same kind of outer-layer structures. In fact, when only wavelengths shorter than $\lambda_x=5\,h$ are considered, the energies of u and w are roughly equal above $y^+=100$, and the three components are equally important at the center of the channel. Otherwise u'^2 is roughly twice w'^2, and three times v'^2, throughout the outer layer. The modes associated with the deep component of the u-spectrum are less prominent in ϕ_{ww}, and are essentially irrelevant in ϕ_{vv}, as could already be inferred from comparing the values given above for C_u, C_v and C_w. This suggests that the mean shear has a direct effect on the generation of the deep u-modes, since the main difference between the three velocity components is that the energy production feeds directly only into u'^2.

The wall-normal organizations of the one-dimensional u-spectrum and of the uv-cospectrum are shown in Fig. 2. They are separated into wavelength bands to isolate the different components mentioned above. The lines separating these bands are shown in Figs. 1(a) and 1(b). Figure 2(a) shows, as functions of λ_x and y, streamwise spectra which are integrated only over wavelengths wider than $\lambda_z = 0.75\,h$. The u-spectrum in this figure has two parts. The long deep u-modes form a vertical ridge at the right of the figure, with a short appendix toward the left at the top of the plot. It can be seen in other decompositions that the latter is a separate peak formed by the quasi-isotropic modes in Fig. 1(b). As y approaches h the deep modes weaken and the quasi-isotropic modes become dominant, in agreement with the assumption that the deep u-modes are directly generated by the mean shear. This may also explain why the one-dimensional u-spectrum measured in pipes moves to shorter wavelengths at the centerline,[6,12] after having become longer across the log-layer. The cospectrum of these wide structures is concentrated away from the wall, but spans both the quasi-isotropic and the long modes, showing that the deep modes are not inactive away from the wall. In Fig. 2(b), which displays the spanwise spectra of all the structures longer than $5\,h$, the deep u-modes can also be seen at the right hand edge of the plot. The diagonal ridge at the bottom of that figure is formed by the long but narrow tail which is seen in Fig. 1(a) along the power-law axis of the near-wall spectrum. This ridge is confined below $y^+ \approx 40$ at both Reynolds numbers.

Both in Fig. 2(b), and in the shorter structures represented in Fig. 2(d), the cospectrum is concentrated along spanwise wavelengths that widen linearly with y. This agrees with the scaling similarity assumption that is used, for example, in deriving the logarithmic law. The same is not true for the u-spectrum, which is known to exhibit incomplete similarity even at very high Reynolds numbers.[13] This is due to the deep long modes which, being global in the wall-normal direction, cannot be involved in any scale similarity with respect to y. In fact, when these modes are removed in Fig. 2(d) the u-spectrum is much closer to self-similarity. The v- and w-spectra, which have weaker deep components, widen approximately linearly with y at all wavelengths.

An attempt to check for streamwise similarity of the narrow scales in Fig. 2(c) fails because there is very little scale separation between the length of the structures near the wall ($\lambda_x^+ \approx 1000$) and those in the outer layer ($\lambda_x \approx 3\,h$). It is not clear from our data whether this is a low-Reynolds number effect, or whether the anisotropy of the near-wall structures will keep increasing with the Reynolds number, preventing streamwise self-similarity from ever developing.

ACKNOWLEDGMENTS

This work was supported in part by the Spanish CICYT Contract No. BFM2000-1468 and by ONR Grant No. N0014-00-1-01416. We are specially indebted to the CEPBA/IBM center of the U. Politècnica de Catalunya, which graciously donated the computer time needed for the simulations.

[1] J. Kim, P. Moin, and R. D. Moser, ''Turbulence statistics in fully developed channel flow at low Reynolds number,'' J. Fluid Mech. **177**, 133 (1987).
[2] R. D. Moser, J. Kim, and N. N. Mansour, ''Direct numerical simulation of turbulent channel flow up to Re_τ=590,'' Phys. Fluids **11**, 943 (1999).
[3] H. Abe, H. Kawamura, and Y. Matsuo, ''Direct numerical simulation of fully developed turbulent channel flow with respect to the Reynolds number dependence,'' J. Fluids Eng. **123**, 382 (2001).
[4] M. Hites, ''Scaling of high-Reynolds number turbulent boundary layers in the National Diagnostic Facility,'' Ph.D. thesis, Illinois Institute of Technology, 1997.
[5] J. Jiménez, ''The largest structures in turbulent wall flows,'' Center for Turbulence Research Annual Research Briefs, Stanford University, 1998.
[6] K. Kim and R. Adrian, ''Very large-scale motion in the outer layer,'' Phys. Fluids **11**, 417 (1999).
[7] J. Jiménez, O. Flores, and M. García-Villalba, ''Organization of autonomous wall turbulence,'' No. 9 in *Advances in Turbulence* (CIMNE, Barcelona, 2002), pp. 825–828.
[8] D. B. De Graaff and J. K. Eaton, ''Reynolds-number scaling of the flat-plate turbulent boundary layer,'' J. Fluid Mech. **422**, 319 (2000).
[9] A. E. Perry and J. D. Li, ''Experimental support for the attached eddy hypothesis in zero pressure gradient boundary layers,'' J. Fluid Mech. **165**, 163 (1990).
[10] A. A. Townsend, *The Structure of Turbulent Shear Flows* (Cambridge University Press, New York, 1976), 2nd ed.
[11] R. J. Adrian, C. D. Meinhart, and C. D. Tomkins, ''Vortex organization in the outer region of the turbulent boundary layer,'' J. Fluid Mech. **422**, 1 (2000).
[12] K. J. Bullock, R. E. Cooper, and F. H. Abernathy, ''Structural similarity in radial correlations and spectra of longitudinal velocity fluctuations in pipe flow,'' J. Fluid Mech. **88**, 585 (1978).
[13] J. F. Morrison, W. Jiang, B. J. McKeon, and A. J. Smits, ''Reynolds-number dependence of streamwise velocity spectra in turbulent pipe flow,'' Phys. Rev. Lett. **88**, 214501 (2002).